

eMotions: A Large-Scale Dataset for Emotion Recognition in Short Videos

Xuecheng Wu¹ Heli Sun^{1*} Junxiao Xue^{2,3} Ruofan Zhai³ Xiangyan Kong⁴ Jiayu Nie¹ Liang He¹
¹Xi'an Jiaotong University ²Zhejiang Lab ³Zhengzhou University ⁴Harbin Institute of Technology

wuxc3@stu.xjtu.edu.cn, hlsun@xjtu.edu.cn

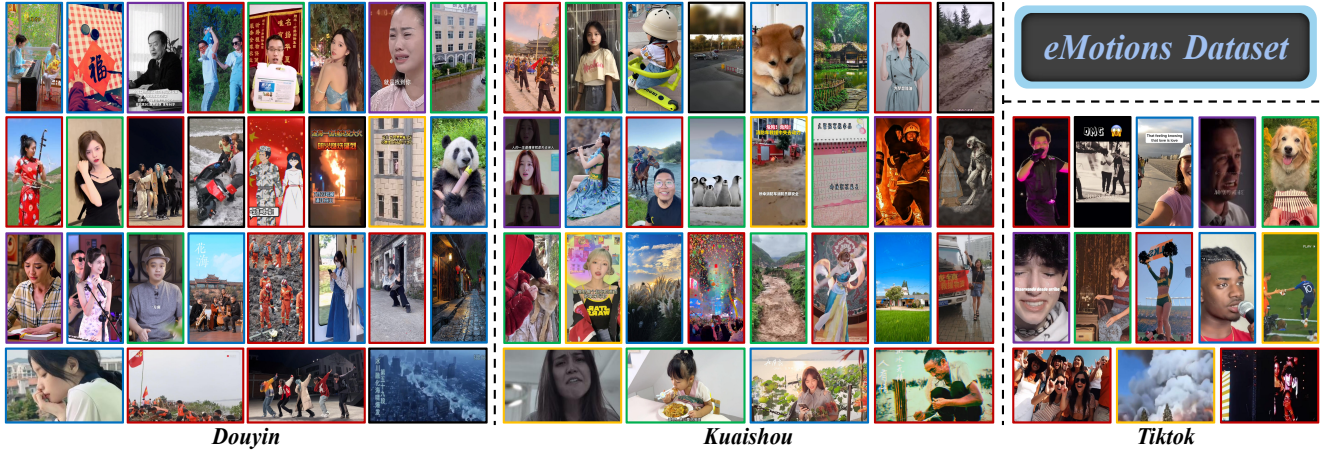


Figure 1. An overview of eMotions composed of 27,996 videos of six emotion categories across Douyin, Kuaishou, and Tiktok. The colors of the frame borders specify the emotion categories to which they belong: **excitation**, **fear**, **neutral**, **relaxation**, **sadness**, **tension**.

Abstract

Nowadays, short videos (SVs) are essential to information acquisition and sharing in our life. The prevailing use of SVs to spread emotions leads to the necessity of emotion recognition in SVs. Considering the lack of SVs emotion data, we introduce a large-scale dataset named eMotions, comprising 27,996 videos. Meanwhile, we alleviate the impact of subjectivities on labeling quality by emphasizing better personnel allocations and multi-stage annotations. In addition, we provide the category-balanced and test-oriented variants through targeted data sampling. Some commonly used videos (e.g., facial expressions and postures) have been well studied. However, it is still challenging to understand the emotions in SVs. Since the enhanced content diversity brings more distinct semantic gaps and difficulties in learning emotion-related features, and there exists information gaps caused by the emotion incompleteness under the prevalently audio-visual co-expressions. To tackle these problems, we present an end-to-end baseline method AV-CPNet that employs the video transformer to better learn semantically relevant representations. We further design the two-stage cross-modal fusion module to complementarily model the correlations of audio-visual features. The EP-CE Loss, incorporating three emotion polarities, is then applied to guide model optimization. Extensive experimental results on nine datasets verify the effectiveness of AV-CPNet. Datasets and code will be open on [GitHub](#).

*Corresponding author.

1. Introduction

Video emotion recognition (VER) is one of the foundational aspects of machine intelligence [67]. It aims to understand the contents of elements and identify which emotion the elements evoke to the viewers. The emotions of viewers can be influenced by various elements, such as videos, audio, text, and images from streaming media [34]. In particular, short videos (SVs), one of the new types of social-media tools, have made rapid progress recently. SVs are concise and clear, combining visual, audio, and other elements to intensify emotional expressions and arouse emotional resonance among viewers, which are crucial to spreading emotions. Therefore, emotion recognition in SVs has significant application values in research fields such as opinion propagation [14], multi-modal LLMs [64], and HCI [47].

Although VER in facial expressions [56, 62] and postures [31] have been well studied, the research in SVs remains light because of the lack of dataset. To tackle this problem and facilitate further studies, we propose a dataset specifically constructed for emotion recognition in SVs, denoted eMotions (Fig. 1), which is the first large-scale dataset in this field. eMotions consists of 27,996 videos with corresponding audio from Douyin, Kuaishou, and Tiktok three SVs platforms, covering various contents across diverse dimensions and totaling 710,881 seconds of duration. Specifically, considering the emotion categories in psychology and the content distribution characteristics of eMotions, we label each sample using the six emotion categories proposed

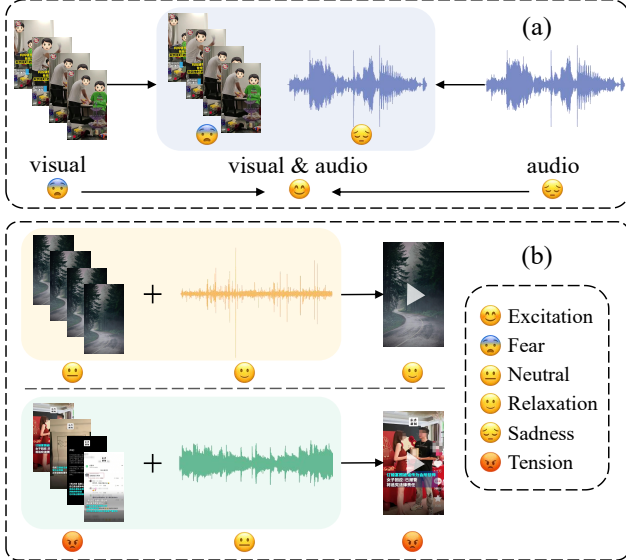


Figure 2. (a) When audio-visual modalities co-express, the emotion which the sample intends to evoke could be reflected. (b) **Top:** The video remains unchanged, and only audio varies over time. **Bottom:** The sample comprises shifting video and less varied audio (e.g., text-to-speech (TTS) voiceovers), in which the audio falls short in expressing emotion.

by Plutchik in [42] (i.e., excitation, fear, neutral, relaxation, sadness, tension). Moreover, to alleviate the impact of subjectivities on labeling quality, we elaborately adjust the personnel allocations through the two-stage Cross-Check and consistencies evaluations, as well as propose a multi-stage annotation workflow. In addition, catering to the class distribution of eMotions and the testing demands, we provide the category-balanced and test-oriented variant datasets.

Compared with traditional VER, emotion recognition in SVs presents unique challenges as follows: As displayed in Fig. 1, the content diversity in SVs is broad, which leads to more distinct semantic gaps and difficulties in learning emotion-related features than commonly used videos. Meanwhile, the emotional information in SVs is prevalently co-expressed through audio-visual modalities and there exists emotion incompleteness which could cause information gaps, as illustrated in Fig. 2. Considering these observations, we analyze three keypoints in the following: (1) Learning more semantically relevant representations and emotion-related features effectively. (2) Deploying the audio-visual joint learning paradigm in an end-to-end manner. (3) Designing efficient fusion module to complementarily facilitate the inter-modalities correlations modeling.

Based on the above keypoints, we present an end-to-end model denoted AV-CPNet (Audio-Visual Cooperatively enhanced Perception Network) as the baseline on eMotions. Unlike previous CNNs-based VER methods [66, 68], we employ Video Swin-Transformer [36] as the visual backbone, which makes our model naturally capture the global relations between regions in each frame and efficiently

model the long-distance dependencies as well as long-term sequences, leading to more semantically relevant representations. The two-stage cross-modal fusion module (TS-CF Module) is designed to mitigate the information gaps, which complementarily captures the correlated information of inter-modalities to output more comprehensive representations. Besides, we propose the EP-CE Loss (Emotion Polarity enhanced Cross-Entropy Loss), which incorporates three emotion polarities (i.e., positive, neutral, negative) to guide model learning more emotion-related features. We conduct extensive experiments comparing the proposed method and existing baseline approaches on six public and three eMotions-related datasets. The results demonstrate the effectiveness of AV-CPNet, suggesting that it could be a potential solution to emotion recognition in SVs.

Our main contributions can be summarized as follows: (1) To our knowledge, eMotions is the first dataset for emotion recognition in SVs. The more reliable annotated emotions can promote future studies in this field. The eMotions and its two variants will be made available to the research community. (2) We propose an effective baseline AV-CPNet to recognize the emotions in SVs. We design the corresponding components to complementarily model the audio-visual correlations and leverage the emotion-polarity information to better guide model optimization. (3) Extensive experimental results on nine datasets verify the superiority of our proposed model and provide detailed insights into different approaches and modalities for future works.

2. Related Works

2.1. Video Emotion Recognition Datasets

AFEW [12] contains 1,809 videos of 330 subjects labeled with seven labels. Aff-Wild2 [29] includes 558 videos with frame-level annotations for valence-arousal estimations. MMI [52] comprises more than 2,900 videos labeled with six emotions, which were captured from lab shooting. FABO [16] consists of approximately 1,900 videos of postures recorded by body cameras. However, these datasets only contain visual modality, which fall short in richness and extensibility. Meanwhile, audio-visual learning has attracted more attention among researchers. As a result, numerous audio-visual VER datasets have emerged. IEMO-CAP [5], the earliest audio-visual VER dataset, originated from lab shooting. EMDb [7] encompasses 52 movie-extracted videos with valence-arousal annotations. NewsRover [13] comprises 929 news-sourced samples categorized under three emotions. VideoEmotion8 [26] and Ekman6 [58] consist of 1,101 and 1,637 videos drawn from video sites. CAER [33] and MELD [49] include 13,201 and 1,433 TV shows-derived videos, respectively. Music_video [40] houses 3,323 music recording videos labeled across six emotions. Compared with these datasets, our eMotions presents the following features: (1) The first dataset for

emotion recognition in SVs, and the currently largest audio-visual VER dataset, exhibiting the escalation of 212.07% and 402.53% compared to the maximum scale and duration of the existing VER datasets, respectively. (2) An emphasis on better personnel allocations and multi-stage annotations to reduce the influence of subjectivities on labeling quality, engaging 12 annotators and one expert. (3) The larger extent of content diversity, sourced from three SVs platforms, covering a multi-cultural spectrum and spanning an extensive timeline from May 2019 to February 2023. (4) We additionally provide two variants of eMotions whose specifics are detailed in appendix.

2.2. Video Emotion Recognition Approaches

Early studies on VER mainly center on designing hand-crafted features [24, 26]. With the emergence of various VER datasets, methods based on deep learning have made rapid progress. For the uni-modal approaches, [3] integrates visual and STAT features to predict emotions. [17] introduces a new 3D CNN for VER using hyper-parameter search. [61] proposes a coarse-to-fine cascaded network with smooth predictions. Regarding the audio-visual VER approaches, they can be widely categorized into two types based on the backbones they employ: those utilizing 3D visual backbones and audio CNNs, and those leveraging 2D visual backbones along with audio CNNs. Pertaining to the first type, 3D visual backbones mainly include [6, 20, 50]. The audio CNNs primarily consist of [15, 22, 30]. [65] proposes a temporal erasing network for keyframe and context perceptions. [66] implements multiple attention mechanisms to output improved audio-visual features. [38] designs an intra-modality attention module to shape attentive features. [18] offers a modality-referenced system using 3D CNNs. [51] provides a pre-trained audio-visual network to model the interactions between human facial and auditory behaviors. [44] introduces a joint model to extract salient features across audio-visual modalities. For the second type, 2D visual backbones primarily comprise [22, 23, 35], with audio CNNs mirroring those employed in the first type. [41] and [60] introduce on-the-fly gradient modulation and a novel cosine loss for enhanced performance, respectively. [9] proposes a framework for incomplete audio-visual data. [43] presents an LSTM-based model adept at capturing contextual information. [46] utilizes the model-level fusion to integrate the visual features extracted by the teacher-student networks with audio features. Besides, [57] utilizes knowledge transfer for VER. [59] offers a fusion framework incorporating concept and content features. [8] unveils a deep semantic feature fusion model. In this paper, we introduce the AV-CPNet, which achieves SOTA performance across three eMotions-related datasets and outcomes promising results on six public datasets, indicating its effectiveness and generalization ability for VER.

3. eMotions Dataset

The overall construction workflow of eMotions is illustrated in Fig. 3 (a), involving data collection and cleaning (Sec. 3.1), personnel assignment and adjustments (Sec. 3.2), multi-stage manual annotation (Sec. 3.3), as well as the expert re-review which purges potential dissensus and biases to further augment labeling quality. Moreover, we conduct labeling quality evaluations (Sec. 3.4) and present the characteristics of eMotions (Sec. 3.5). Besides, we build two variant datasets through targeted sampling.

3.1. Data Collection and Cleaning

We deploy the web crawler to collect hot events, which are diverse and representative, as the raw data. Meanwhile, we carry out a stage-by-stage crawling strategy interleaved with the formal annotation to ensure an extensive timeline. During data cleaning, identical and corrupted videos are removed, and videos containing racial discrimination, violence, and pornography are also eliminated to reduce the ethical biases of our trained models. Furthermore, considering the specificities of categorical emotions, videos featuring consecutive emotional shifts are also discarded.

3.2. Personnel Assignment and Adjustments

Each annotator is asked first to pass the labeling test, comprising the sentiment quotient test and the annotation quality evaluation [34, 63]. When scoring 90 or above in accuracy, the annotators can join in the emotion labeling. We then hold training sessions for them, including the detailed workflow and targeted learning on multi-cultures.

Assignment: As formulated in Eq. 1, we consider five important factors to determine the assignment of group members and leaders, which can promote collaborations among annotators and benefit future adjustments. Besides, each group consists of two male and one female members to balance the gender distribution.

$$p = 0.4 \cdot we + 0.3 \cdot ms + 0.1 \cdot (eb + cb + lp) \quad (1)$$

where we , eb , cb , and lp denote the work experiences, education backgrounds, cultural backgrounds, and leaderships, respectively. For MSCEIT [37] scores (ms), higher ranking indicates better emotion cognition.

Adjustments: We perform personnel adjustments following assignment to alleviate the impact of subjectivities on the annotations employing the multi-groups with multi-annotators, which are reflected in the improvements of the consistencies of intra-group and inter-group (*i.e.*, S_a , S_r) [32]. Specifically, we select 9,000 samples from the cleaned data and distribute them evenly among the assigned groups. GroupA (GA), GroupB (GB), and GroupC (GC) are each requested to perform annotation following the workflow described in Sec. 3.3, and the leaders here only carry out results collection. We then sample 18 sets from the annotations of each group to conduct two-stage Cross-Check

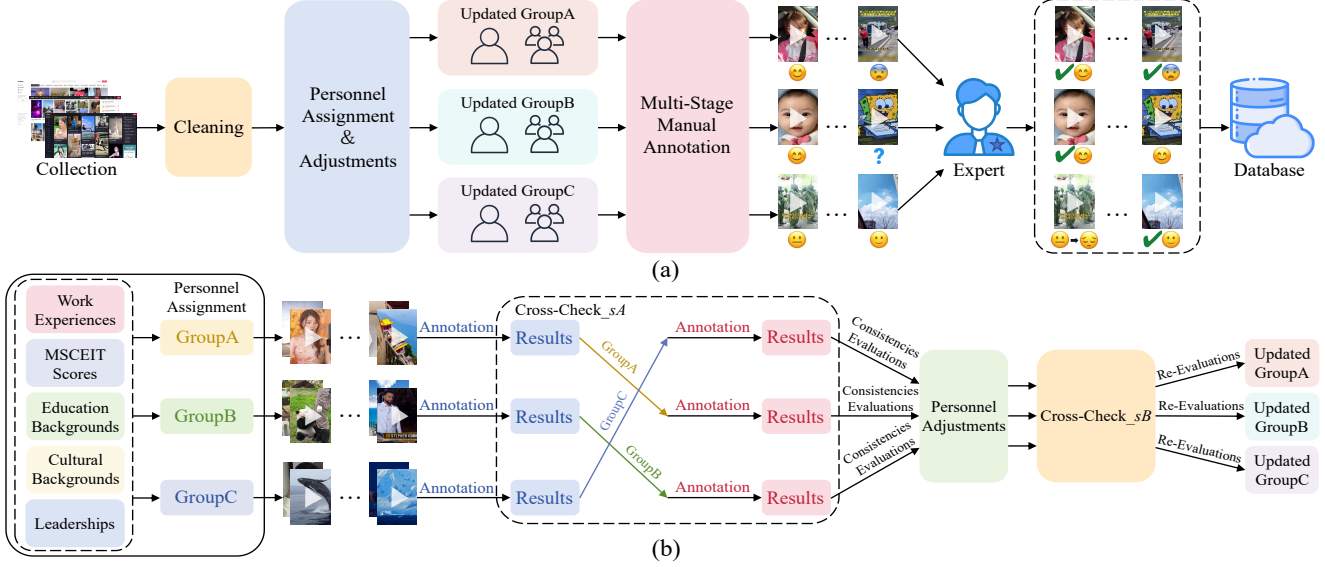


Figure 3. (a) The overall illustration of the construction workflow of eMotions. (b) The pipeline of personnel assignment and adjustments.

Table 1. The evaluation results of consistencies of intra-group and inter-group (S_a and S_r) following Cross-Check.

Stage	GroupA		GroupB		GroupC	
	S_a	S_r	S_a	S_r	S_a	S_r
sA	0.52	52.55	0.53	48.78	0.55	54.54
sB	0.55	55.53	0.56	54.41	0.56	55.79

[1, 19], in which we first exchange the annotations of three groups in pairs and then annotate these samples again, as illustrated in Fig. 3 (b). These sets, each including 100 samples, are equally divided into two parts for two-stage Cross-Check (*i.e.*, sA , sB). Each stage has three sets for neutral, two sets for excitation, and one set for each of sadness, relaxation, tension, as well as fear. Subsequently, we evaluate the consistencies of intra-group and inter-group under the present allocations based on the results of Cross-Check_{sA}. The ranges of S_a and S_r formulated as Eq. 2 and Eq. 3 are from 0 to 1 and 0 to 70, respectively. The larger S_a and S_r indicate the increasing consistencies.

$$S_a = \frac{1}{n} \cdot \sum_{i=0}^{n-1} \left(\frac{1}{3 \cdot m} \cdot \sum_{j=1}^m c_j \right) \quad (2)$$

$$S_r = \frac{1}{c} \sum_{i=0}^{n-1} w_i \cdot (0.7 \cdot C_i + 0.3 \cdot (m - C_i - M_i)) \quad (3)$$

where n , m , and c denote the number of sets, samples per set, and emotion categories, respectively. c_j refers to the quantity of currently annotated categories of three annotators for one sample that are consistent with the previous category. $w_i \in \{\frac{1}{3} | 0 \leq i < 3, \frac{1}{2} | 3 \leq i < 5, 1 | 5 \leq i \leq 8\}$ represents the weight coefficient for each set, depending on the number of sets in each category. C_i stands for the samples consistent with previous annotations. M_i denotes the “more” samples, indicating the final label is indeterminate.

Table 2. The newly proposed mapping table of emotion-category-to-adjective, comprising 62 adjectives.

Category	Adjectives
Excitation	Happy, Fun, Sexy, Joyful, Pleasant, Exciting, Adorable, Cheerful, Surprising, Interesting, Active, Hopeful, Enjoyable, Lively, Loving, Spirited, Touching
Fear	Horrific, Fearful, Scary, Dreadful
Neutral	Little (Sad, Fearful, Exciting, Relaxing, Happy, Tensed), Insensitive, Indifferent, Narrative, Unsentimental, Mind-numbing
Relaxation	Calm, Tranquil, Leisure, Peaceful, Soothing, Relaxing, Stress-releasing
Sadness	Depressing, Chilling, Sentimental, Shameful, Distressed, Anguished, Melancholic, Heart-breaking, Sorrowful, Regrettable, Heart-wrenching, Agonizing, Sympathetic
Tension	Angry, Hateful, Panicking, Raging, Tensed, Fast-paced, Accelerated, Anxious, Disturbing, Flustered

As shown in Tab. 1, S_a of the three groups achieve 0.52, 0.53, and 0.55, respectively. S_r stand at 52.55, 48.78, and 54.54, with GB scoring relatively low. Considering these observations, we perform targeted adjustments, then re-evaluate the consistencies after Cross-Check_{sB}. Following adjustments, S_a of GA and GB each rise by 0.03, and that of GC improves by 0.01. S_r of three groups increase by 2.98, 5.63, and 1.25, where GB exhibits the highest improvement. These results verify the effectiveness of our adjustments, indicating that we have finalized the personnel allocations that can be deployed for formal annotation. Note that the overall results of two-stage Cross-Check and the pseudocode of adjustments strategy are detailed in appendix.

3.3. Multi-Stage Manual Annotation

The multi-stage manual annotation workflow combines member votes and leader evaluations, benefiting to reduce the impact of subjectivities. We further propose a mapping table of emotion category-to-adjective to promote annotations, as displayed in Tab. 2. Besides, we have developed a

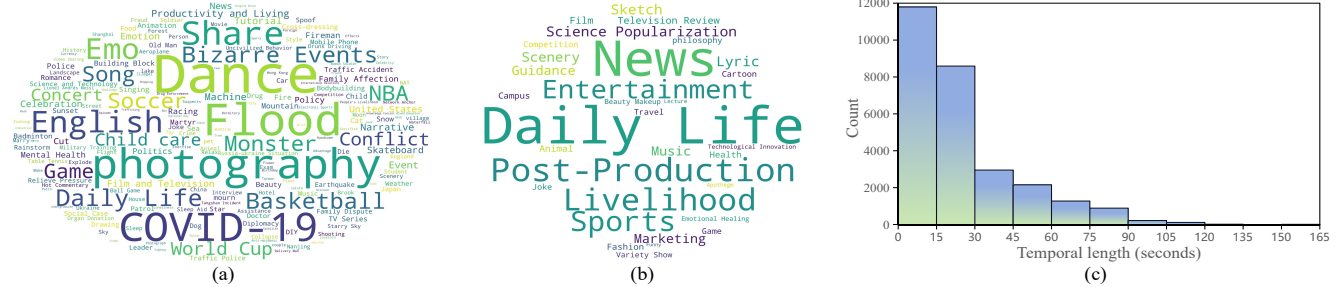


Figure 4. (a) & (b) Word clouds of topics and content types in eMotions. Larger text size indicates a higher frequency of occurrence. (c) Duration distribution of short videos in our dataset.

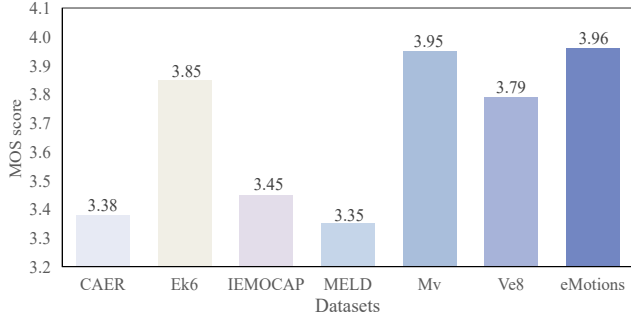


Figure 5. The MOS scores of six existing VER datasets and our eMotions. Specifically, Ek6, Mv, and Ve8 refer to Ekman6 [58], Music_video [40], and VideoEmotion8 [26], respectively.

labeling interface to boost the stimulation and engagement of annotators. Specifically, the leader distributes data, followed by three members undertaking annotations via the proposed mapping table. Meanwhile, members are asked to attach confidence scores to their annotations, and the average score finally stands at 0.7. Next, the leader collects these annotations, leveraging a majority voting scheme to determine labels. If annotations from three members are all different (*i.e.*, samples labeled “more”), the leader will intervene in labeling. If a decisive majority of four votes emerges, the final labels can be directly determined. If consensus is still challenging to reach, leaders will exchange samples to facilitate decision-making. In five votes, a clear majority allows to determine the final labels. If consensus continues to be inaccessible, the expert will finalize the labels in re-review. After completing the annotations, we calculate the overall Fleiss’kappa score and achieve $k > 0.45$.

3.4. Labeling Quality Evaluations

In this section, we conduct labeling quality evaluations for proposed eMotions and six public VER datasets. Specifically, we first perform the random sampling of seven datasets, totaling 979 samples, based on the sample correction formula proposed in [48]. We then employ four emotional annotation experts to independently evaluate the labeling quality of these datasets. The MOS scores [45] are utilized as our evaluation metrics, in which the ratings from 1 to 5 represent the five levels of quality (*i.e.*, bad, poor, fair, good, excellent). Next, for each dataset, we average the assessments of four experts and regard the output as the final

Table 3. The statistics of eMotions, detailing the number of videos and processed frames for each category, along with the quantitative durations. The magnitude is 10^4 for “Total (s)” and “Frames”.

Category	Videos	Total (s)	Shortest (s)	Longest (s)	Average (s)	Frames
Excitation	11739	29.35	3.72	163.77	25.00	945.29
Fear	954	2.59	2.81	117.49	27.08	78.56
Neutral	8795	24.97	2.46	150.93	28.39	815.11
Relaxation	2214	5.24	5.06	117.05	23.69	163.80
Sadness	2090	4.04	3.25	120.77	19.30	131.53
Tension	2204	4.90	3.79	119.32	22.25	152.15
Overall	27996	71.09	2.46	163.77	25.39	2286.44

Table 4. The quantity and proportions of raw and labeled data across the three SVs platforms of Douyin, Kuaishou, and Tiktok.

Data Type	Douyin		Kuaishou		Tiktok		Sum
	No.	Ratio	No.	Ratio	No.	Ratio	
Raw	15977	47.58%	10000	29.78%	7600	22.64%	33577
Labeled	12395	44.27%	8264	29.52%	7337	26.21%	27996

rating. Although the videos in Music_video [40] originating from music recordings are easier to evoke emotions than those from other sources (*e.g.*, video sites, SVs), our eMotions exhibits the highest rating, indicating the more reliable labeling quality than existing VER datasets, as illustrated in Fig. 5. The above observations demonstrate the effectiveness of reducing the impact of subjectivities and performing the expert re-review to augment labeling quality.

3.5. Dataset Characteristics

We show the statistics of eMotions in Tab. 3, including the number of videos and processed frames for each category, as well as the statistical durations. We can see that excitation has the largest number of videos, while the negative emotions (*i.e.*, fear, sadness, tension) have the smaller number of videos. In Tab. 4, we present the quantity and proportions of raw and labeled data across three SVs platforms. We figure out that videos from Douyin and Kuaishou, two Chinese SVs platforms, account for the largest proportion.

We display the word clouds of topics and content types in Fig. 4 (a) and Fig. 4 (b). It can be seen that the topics mainly focus on daily events in life, such as dance and photography, as well as the real-time events, such as COVID-19, floods, and 2022 FIFA World Cup. Content types are closely connected to human beings (*e.g.*, daily life, livelihood, news). Moreover, some topics and content types of SVs are consis-

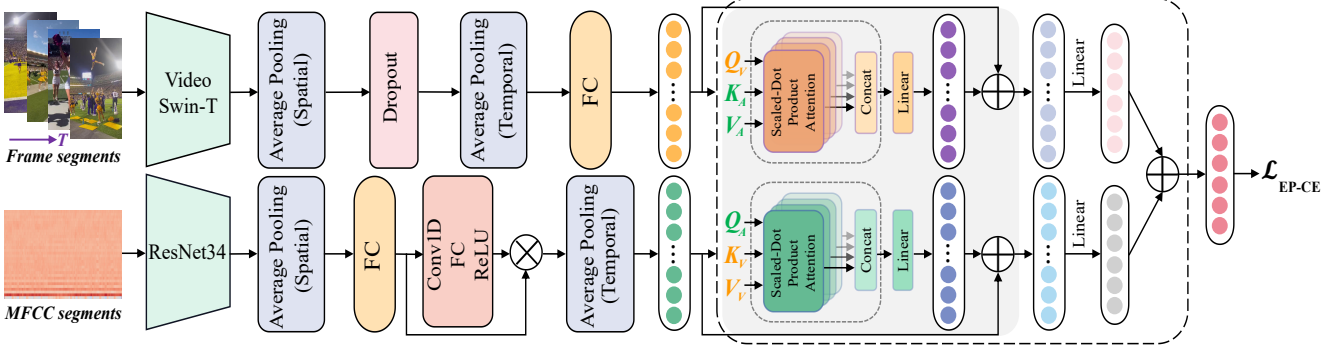


Figure 6. The overall architecture of AV-CPNet. Specifically, Conv1D and FC respectively denote 1×1 convolution and Fully Connected Layer. Note that the components framed with dashed lines are our proposed TS-CF Module.

tent (e.g., game, health). Fig. 4 (c) presents the distribution of SVs duration. We find that the durations mainly concentrate from 0 to 30 seconds, taking up 72.81% of the overall dataset. This indicates that SVs are concise which can meet the needs of users for quick information dissemination.

4. Methodology

4.1. Visual and Audio Representations

To tackle the inherent challenges of SVs, we end-to-end extract audio-visual representations. Unlike [65, 66], we employ the Video Swin-Transformer (Video Swin-T) [36] as the visual backbone since it can effectively capture more semantically relevant features. Specifically, let $\{(v_i, a_i)\}^b$ be a batch of b samples, in which v_i, a_i denote the video and audio in i -th sample. For v_i , we first divide it into s segments of equal duration and randomly select a snippet of k consecutive frames from each segment. We then sample T frames from each snippet and take s snippets as the input. For each segment-level input $v_i^j \in \mathbb{R}^{T \times H \times W \times 3}$, we first project it into the patch features $v_i^j \in \mathbb{R}^{\frac{T}{2} \times \frac{H}{4} \times \frac{W}{4} \times 96}$, where H and W indicate the height and width of v_i . For the l -th stage in Video Swin-T, the input features can be represented as $F_v^l = \frac{T}{2} \times \frac{H}{2^{l+1}} \times \frac{W}{2^{l+1}} \times 2^{l-1} C$, $l \in \{1, 2, 3, 4\}$. Specifically, for the first stage, a linear embedding layer is applied to project the patch features to the dimension C . The patch merging layers are utilized in the remaining stages to progressively reduce the spatial size of feature maps. In each Video Swin-T block, F_v^l is transformed into *query*, *key*, and *value* embeddings, respectively. Moreover, the blocks deploy the 3D SW-MSA module which does not change the shape of feature maps, to capture global relations and model spatial-temporal correlations. After processing, the final representations of v_i comprise a series of segment features $F_v(v_i) = f_v^1(v_i), \dots, f_v^s(v_i)$, and $f_v^j(v_i) \in \mathbb{R}^{\frac{T}{2} \times \frac{H}{32} \times \frac{W}{32} \times 8C}$.

For audio a_i , we obtain a successive descriptor a through MFCC. We then center-crop a to a fixed length of q and pad itself when necessary to get a' . Next, we divide a' into t segments, and utilize the ResNet34 [22] to output the final representations $F_a(a_i) = f_a^1(a_i), \dots, f_a^t(a_i)$, and $f_a^p(a_i) \in$

$\mathbb{R}^{H' \times W' \times C'}$, in which H' , W' , and C' denote the height, width, and final dimension, respectively.

Subsequently, we deploy pooling layers along the spatial and temporal dimensions, followed by a fully connected layer to reshape F_v as $F_v^1 \in \mathbb{R}^{C_1}$. We then apply spatial pooling and a fully connected layer to reshape F_a as $F_a^1 \in \mathbb{R}^{l \times C_1}$, and deploy a temporal attention module (i.e., 1×1 convolution, fully connected layer, ReLU layer) to enhance the temporal representations, followed by temporal pooling to reshape it as $F_a^2 \in \mathbb{R}^{C_1}$.

4.2. Two-Stage Cross-Modal Fusion

We design a two-stage cross-modal fusion module (TS-CF Module), which consists of Cross-Attention Fusion Layer (CAF Layer) and SumFusion Layer (SF Layer), to complementarily bridge the information gaps caused by the emotion incompleteness in SVs. In Sec. 4.1, we reshape the features and adjust them to the same dimension, which can efficiently provide representations with higher information density, avoiding the impact of redundant information on correlations modeling of audio-visual features. To adapt the following procedures, we then transform F_v^1 and F_a^2 to $F'_v \in \mathbb{R}^{l \times C_1}$ and $F'_a \in \mathbb{R}^{l \times C_1}$ by unsqueezing.

Next, the multi-head self-attention (MHSA) layers are adopted and the *queries* (Q) of F'_v and F'_a are F'_v and F'_a , while both the *keys* (K) and *values* (V) of F'_v and F'_a are F'_a and F'_v , respectively. This allows F'_v and F'_a to search each other for the correlations with the other modality. The four self-attention heads in MHSA layer can form four separate feature spaces to learn representations at various levels and different degrees of correlations. Subsequently, the non-local aggregations of features are performed through concatenating to output more comprehensive audio-visual representations (i.e., F'_{v_1} and F'_{a_1}). These operations formulated as Eq. 4 and Eq. 5 in the CAF Layer enable our AV-CPNet to complementarily model the inter-modalities correlations, thus effectively mitigating the information gaps. Note that $1/\sqrt{d_k}$ in Eq. 4 is the scaling factor.

$$Att(Q, K, V) = \text{softmax} \left(QK^T / \sqrt{d_k} \right) V \quad (4)$$

$$MHSA(Q, K, V) = \text{concat} (Att_1, \dots, Att_4) W^O \quad (5)$$

Table 5. Performance comparisons of AV-CPNet and various kinds of advanced baseline methods on six public and three eMotions-related datasets in terms of Acc (%) and WA-F1. Specifically, Mod., e_B , and e_T denote Modality, eMotions.balanced, and eMotions.test, respectively. † indicates that AV-CPNet is initialized using the weight learned from eMotions. Note that “-” means the experimental results are not available due to inaccessible code.

Method	Mod.	CAER		Ek6		IEMOCAP		MELD		Mv		Ve8		e_B		e_T		eMotions	
		Acc	WA-F1	Acc	WA-F1	Acc	WA-F1	Acc	WA-F1	Acc	WA-F1	Acc	WA-F1	Acc	WA-F1	Acc	WA-F1	Acc	WA-F1
ResNet34 [22]	Audio	36.28	28.87	33.95	32.17	38.89	36.45	46.56	32.45	72.73	73.07	31.63	29.11	50.71	49.66	55.10	51.95	59.14	58.41
PANNS [30]	Audio	35.48	24.20	27.47	21.77	40.30	34.85	47.37	34.24	63.38	61.46	27.91	23.06	51.02	50.36	50.50	45.09	58.34	55.99
Res2Net [15]	Audio	35.98	29.86	31.17	29.64	37.67	34.66	45.63	29.03	65.91	65.76	29.77	27.12	49.15	47.56	50.80	46.76	55.43	52.15
CAMPPlus [55]	Audio	26.34	26.53	29.01	29.03	40.65	39.07	27.22	30.23	70.71	71.79	22.33	23.59	53.27	53.17	52.10	52.38	56.48	57.06
Video Swin-Transformer [36]	Visual	56.81	55.77	47.59	49.44	58.16	58.13	45.99	29.48	74.68	80.64	46.31	45.77	61.48	63.53	63.20	62.79	64.64	66.02
I3D [6]	Visual	48.24	46.00	40.51	42.10	56.75	52.60	45.93	28.99	64.05	79.75	40.89	41.34	56.02	62.79	60.10	59.90	63.14	65.00
Ji et al. [25]	Visual	52.10	-	41.30	-	-	-	-	-	-	-	39.30	-	-	-	-	-	-	-
TimeSformer [4]	Visual	56.39	53.25	36.33	34.34	26.75	14.71	45.93	29.14	78.23	81.07	46.30	45.65	63.28	63.93	62.70	61.59	63.66	64.48
C3D [50]	Visual	53.01	54.51	44.05	42.84	60.53	59.63	45.99	28.85	62.78	77.43	42.36	42.02	56.15	60.77	59.10	60.00	62.18	63.86
Chen et al. [8]	E+O+S	-	-	51.80	-	-	-	-	-	-	-	50.60	-	-	-	-	-	-	-
Xu et al. [59]	E+O+S	-	-	51.20	-	-	-	-	-	-	-	51.40	-	-	-	-	-	-	-
ITE [57]	T+V	-	-	50.90	-	-	-	-	-	-	-	43.80	-	-	-	-	-	-	-
Pandeya et al. [40]	A+V	-	-	-	-	-	-	-	-	70.94	70.00	-	-	-	-	-	-	-	-
I3D [6] +1D Music CNN [39]	A+V	-	-	-	-	-	-	-	-	69.78	69.00	-	-	-	-	-	-	-	-
VAA-Net [66]	A+V	41.26	35.86	50.31	49.65	53.77	51.55	45.22	34.79	78.99	77.99	46.73	43.92	60.01	59.89	60.10	59.46	63.71	63.30
Jiang et al. [26]	A+V	-	-	-	-	-	-	-	-	-	-	46.10	-	-	-	-	-	-	-
3D-ResNet50 [20] + ResNet34 [22]	A+V	41.64	35.14	48.44	47.57	49.04	48.07	34.87	33.64	73.42	72.98	44.39	43.21	62.53	62.31	60.20	59.04	63.98	63.44
ConvNext [35] +CSPNet [54]	A+V	38.83	33.32	50.00	49.33	44.91	42.67	33.38	33.80	75.70	74.25	45.33	45.23	62.91	62.87	63.20	62.33	64.21	63.58
+Bi-LSTM	A+V	-	-	-	-	-	-	-	-	-	-	-	-	-	-	-	-	-	-
CIM [2]	T+V+A	-	-	-	-	56.93	56.14	-	-	49.13	48.56	-	-	-	-	-	-	-	-
COGMEN [27]	T+V+A	-	-	-	-	-	-	-	-	52.23	52.32	-	-	-	-	-	-	-	-
CMN [21]	T+V+A	-	-	-	-	56.32	56.19	-	-	-	-	-	-	-	-	-	-	-	-
AV-CPNet	A+V	46.76	44.02	53.12	52.57	57.37	56.63	47.48	34.85	81.52	81.38	47.66	45.81	63.81	63.98	65.80	65.01	67.08	66.45
AV-CPNet†	A+V	48.88	47.88	53.44	53.71	58.60	57.81	48.03	39.54	83.04	82.78	51.40	51.18	-	-	-	-	-	-
		(+2.12)	(+3.86)	(+0.32)	(+1.14)	(+1.23)	(+1.18)	(+0.55)	(+4.69)	(+1.52)	(+1.40)	(+3.74)	(+5.37)	-	-	-	-	-	-

Afterwards, we transform F'_{v_1} and F'_{a_1} to the original shapes using poolings and deploy the linear layers to adaptively adjust the weighted audio-visual features, enhancing the focus on key information. Following [36, 53], we also apply the residual connection to benefit the free information flow between layers and promote the gradient propagation.

$$F'_{v_2} = \delta(\sigma(F'_{v_1})) + F'_v \quad (6)$$

$$F'_{a_2} = \delta(\sigma(F'_{a_1})) + F'_a \quad (7)$$

where $\sigma(\cdot)$ and $\delta(\cdot)$ denote the average pooling and linear transformation, respectively.

In the SF Layer, we employ two fully connected layers for dimension adjustments, and then integrate the audio-visual features by sumfusion to output the final representations of the overall model, as formulated in Eq. 8.

$$F_f = \delta_1(F'_{v_2}) + \delta_1(F'_{a_2}) \quad (8)$$

4.3. Emotion Polarity Enhanced CE Loss

Directly optimizing the traditional CE Loss could result in misclassification due to the more significant semantic gaps and difficulties in learning emotion-related features. Inspired by [10, 66], we develop the EP-CE Loss, which further considers the *neutral* polarity commonly presented in CES based VER datasets [33, 40, 58]. Specifically, when the emotion polarity of prediction is different from the ground-truth, the $\gamma_{ep(y_i)}$ will function to weight the model optimization. The EP-CE Loss is defined as follows:

$$\mathcal{L}_{ep} = -\frac{1}{N} \sum_{i=1}^N (1 + \gamma_{ep(y_i)} \cdot s(y_i, \hat{y}_i)) \sum_{c=0}^{C-1} \alpha_{[c=y_i]} \log p_{i,c} \quad (9)$$

where C is the number of categories. $\alpha_{[c=y_i]}$ is a binary indicator, and $p_{i,c}$ is the predicted probability that sample i belongs to category c . $\gamma_{ep(y_i)}$ refers to the coefficients

for polarities that control the penalty extents. y_i and \hat{y}_i denote the ground-truth and the prediction. $s(y_i, \hat{y}_i)$ represents whether to add the penalties. When $ep(y_i) \neq ep(\hat{y}_i)$, $s(y_i, \hat{y}_i) = 1$, otherwise $s(y_i, \hat{y}_i) = 0$, where $ep(\cdot)$ maps the emotion category to its corresponding polarity.

Furthermore, to capture more global features and reduce over-fitting, we adopt the multi-task learning strategy for AV-CPNet on eMotions, which is defined as follows:

$$\mathcal{L}_{sum} = \mathcal{L}_{ep}^f + \mathcal{L}_{ep}^v + \mathcal{L}_{ep}^a \quad (10)$$

where \mathcal{L}_{sum} , \mathcal{L}_{ep}^f , \mathcal{L}_{ep}^v , and \mathcal{L}_{ep}^a refer to the losses for overall, fusion, visual, and audio outputs, respectively.

5. Experiments

5.1. Performance Comparisons

Tab. 5 compares our AV-CPNet with 21 baseline methods on nine datasets, in which the modalities of compared approaches include audio, visual, event-object-scene (E+O+S), text-visual (T+V), audio-visual (A+V), and text-visual-audio (T+V+A). We can draw the following observations: (1) Visual features dominate VER compared to the audio counterparts, and the stronger visual backbone generally leads to more performance gains. (2) AV-CPNet is well-designed and practical, which can adeptly recognize the emotions in SVs. Our model achieves SOTA performance across three eMotions-related datasets, exhibiting the highest improvement of 5.70% Acc and 5.55 WA-F1. (3) AV-CPNet has superior robustness and generalization ability for various applications-oriented VER, performing favorably against the baseline approaches on six public datasets (More analysis is detailed in appendix).

As illustrated in Tab. 5, we further investigate the impact of the more reliable annotations of eMotions on model performance across six existing datasets by initializing AV-

Table 6. Performance comparisons of different weights for AV-CPNet initialization in terms of Acc (%) and WA-F1 on $e.T$.

$e.T$	Different Sources of Weights for Initialization						
	ImageNet	CAER	Ek6	IEMOCAP	MELD	Mv	Ve8
Acc	65.80	64.80	64.90	62.20	64.60	64.90	63.70
WA-F1	65.01	63.79	64.26	61.45	63.36	64.04	62.53

Table 7. The ablation study results of AV-CPNet on three datasets.

Method	eMotions		Music_video		Ekman6	
	Acc	WA-F1	Acc	WA-F1	Acc	WA-F1
Baseline [66]	63.71	63.30	78.99	77.99	50.31	49.65
Audio	59.14	58.41	72.73	73.07	33.95	32.17
Visual	64.64	66.02	74.68	80.64	47.59	49.44
Audio + Visual	65.98	65.05	75.19	74.66	50.31	50.41
+ CAF Layer	66.51	66.14	80.51	80.22	51.25	50.03
+ SF Layer	66.80	66.26	80.52	79.92	52.50	52.02
+ EP-CE Loss	67.08	66.45	81.52	81.38	53.12	52.57

CPNet with the weight learned from eMotions. We figure out that as compared to when loaded with the original weights from ImageNet [11], AV-CPNet achieves superior performance across all the six VER datasets. This indicates that the more reliable annotated emotions can assist models in determining more precise feature mappings and understanding various elements for emotional expressions.

To verify whether the existing datasets are suitable for emotion recognition in SVs, we initialize AV-CPNet with weights learned from six VER datasets and [11], and then conduct comparisons on $e.T$, as shown in Tab. 6. When loading the original weights from [11], AV-CPNet performs best, suggesting that despite the existing datasets containing more emotion-related information, they are inappropriate for the SVs application scenario. The outcomes verify the necessity of constructing a dedicated dataset for SVs.

5.2. Ablation Study

We investigate the components of AV-CPNet by ablation study, as displayed in Tab. 7. (1) We first examine the influence of audio and visual branches, and the results underscore the significance of visual features in audio-visual VER. (2) We then analyze the effect of adopting the audio-visual joint learning paradigm. The outcomes suggest that the joint manner generally benefits models learning richer features, advancing to model the inter-modalities correlations. (3) Next, we investigate the impact of the CAF Layer in promoting complementary learning for audio-visual features. Our AV-CPNet exhibits the largest improvement of 5.32% Acc and 5.56 WA-F1, confirming that the capability of complementary learning is crucial for effectively shaping correlated representations to mitigate the information gaps. (4) We further study the effect of the SF Layer, delivering the highest enhancement of 1.25% Acc and 1.99 WA-F1. Moreover, as shown in Tab. 8, we conduct the ablation comparisons of different fusion strategies, demonstrating that sumfusion is more appropriate for audio-visual VER. (5) Finally, we apply EP-CE Loss to guide model optimization.

Table 8. The ablation comparisons of five different fusion strategies in TS-CF Module. Note that ‘‘EW’’ refers to Element-Wise.

Fusion Strategy	eMotions		Music_video		Ekman6	
	Acc	WA-F1	Acc	WA-F1	Acc	WA-F1
ConcatFusion	66.51	66.14	80.51	80.22	51.25	50.03
EW-SumFusion	65.78	65.18	78.23	78.07	48.13	47.22
NeuralFusion	66.03	65.69	77.47	77.45	49.69	48.81
GatedFusion [28]	65.65	64.64	76.20	75.59	52.19	51.29
SumFusion	66.80	66.26	80.52	79.92	52.50	52.02

Table 9. The ablation comparisons of five different penalties for the EP-CE Loss. Note that γ_{neu} doesn’t function on Ekman6.

$\gamma_{pos} : \gamma_{neu} : \gamma_{neg}$	eMotions		Music_video		Ekman6	
	Acc	WA-F1	Acc	WA-F1	Acc	WA-F1
0 : 0 : 0	66.80	66.26	80.52	79.92	52.50	52.02
0 : 0.3 : 0.5	66.57	65.90	80.62	79.94	51.56	51.04
0.3 : 0.3 : 0.3	66.94	66.39	80.00	79.39	52.81	52.20
0.4 : 0.4 : 0.4	66.10	65.67	80.01	80.01	49.38	48.83
0.5 : 0.5 : 0.5	67.08	66.45	81.52	81.38	53.12	52.57

The results indicate that deploying EP-CE Loss can assist the models in learning more emotion-related features.

Tab. 9 records the ablation comparisons for the emotion polarities with different penalties. It can be seen that AV-CPNet on three datasets consistently performs best when $\gamma_{ep(y_i)} = 0.5$. We thus conclude that under this combination, AV-CPNet with a more balanced weight distribution can potentially exhibit performance improvements, preventing training instabilities. Besides, these observations suggest that the performance improvements sensitively depend on the penalties for different polarities.

6. Conclusion and Prospects

In this paper, we propose the first dataset for emotion recognition in SVs, denoted eMotions. It comprises 27,996 videos labeled across six emotions, sourcing from three SVs platforms. Meanwhile, we make efforts to augment the labeling quality by alleviating the influence of subjectivities. Additionally, two variant datasets are provided through targeted data selections. We also develop a baseline model AV-CPNet to tackle the inherent challenges of emotion recognition in SVs. Extensive experimental results on nine datasets verify the superiority of our AV-CPNet. We hope this work can serve as a foundation and inspire more research.

The granular divisions of audio promote to output more refined representations, and the utilization of text overlays in SVs could assist models in understanding emotions, both indicating the potential development directions of eMotions. Considering the long-tail distribution presented in eMotions, we have proposed the category-balanced variant. However, we still need to purposefully design deep models and learning strategies. Furthermore, the abundant emotional information embedded in eMotions can facilitate the multi-modal alignments of LLMs with the emotional behaviors of human beings, heightening the emotional robustness of LLMs and relevant multi-agent systems.

7. Acknowledgements

eMotions and its two variants will not be transferred to outside parties without permissions and can be utilized only for academic research purposes. In particular, the datasets will not be included as part of any commercial software package or product of any institution.

References

- [1] Gavin Abercrombie, Verena Rieser, and Dirk Hovy. Consistency is key: Disentangling label variation in natural language processing with intra-annotator agreement. *arXiv preprint arXiv:2301.10684*, 2023. 4
- [2] Md Shad Akhtar, Dushyant Singh Chauhan, Deepanway Ghosal, Soujanya Poria, Asif Ekbal, and Pushpak Bhattacharyya. Multi-task learning for multi-modal emotion recognition and sentiment analysis. *arXiv preprint arXiv:1905.05812*, 2019. 7
- [3] Sarah Adel Bargal, Emad Barsoum, Cristian Canton Ferrer, and Cha Zhang. Emotion recognition in the wild from videos using images. In *Proceedings of the 18th ACM International Conference on Multimodal Interaction*, pages 433–436, 2016. 3
- [4] Gedas Bertasius, Heng Wang, and Lorenzo Torresani. Is space-time attention all you need for video understanding? In *ICML*, volume 2, page 4, 2021. 7
- [5] Carlos Busso, Murtaza Bulut, Chi-Chun Lee, Abe Kazemzadeh, Emily Mower, Samuel Kim, Jeannette N Chang, Sungbok Lee, and Shrikanth S Narayanan. Iemocap: Interactive emotional dyadic motion capture database. *Language resources and evaluation*, 42:335–359, 2008. 2
- [6] Joao Carreira and Andrew Zisserman. Quo vadis, action recognition? a new model and the kinetics dataset. In *proceedings of the IEEE Conference on Computer Vision and Pattern Recognition*, pages 6299–6308, 2017. 3, 7
- [7] Sandra Carvalho, Jorge Leite, Santiago Galdo-Álvarez, and Oscar F Gonçalves. The emotional movie database (emdb): A self-report and psychophysiological study. *Applied psychophysiology and biofeedback*, 37:279–294, 2012. 2
- [8] Chen Chen, Zuxuan Wu, and Yu-Gang Jiang. Emotion in context: Deep semantic feature fusion for video emotion recognition. In *Proceedings of the 24th ACM international conference on Multimedia*, pages 127–131, 2016. 3, 7
- [9] Kateryna Chumachenko, Alexandros Iosifidis, and Moncef Gabbouj. Self-attention fusion for audiovisual emotion recognition with incomplete data. In *2022 26th International Conference on Pattern Recognition (ICPR)*, pages 2822–2828. IEEE, 2022. 3
- [10] Yin Cui, Menglin Jia, Tsung-Yi Lin, Yang Song, and Serge Belongie. Class-balanced loss based on effective number of samples. In *Proceedings of the IEEE/CVF conference on computer vision and pattern recognition*, pages 9268–9277, 2019. 7
- [11] Jia Deng, Wei Dong, Richard Socher, Li-Jia Li, Kai Li, and Li Fei-Fei. Imagenet: A large-scale hierarchical image database. In *2009 IEEE conference on computer vision and pattern recognition*, pages 248–255. Ieee, 2009. 8
- [12] Abhinav Dhall, Amanjot Kaur, Roland Goecke, and Tom Gedeon. Emotiw 2018: Audio-video, student engagement and group-level affect prediction. In *Proceedings of the 20th ACM International Conference on Multimodal Interaction*, pages 653–656, 2018. 2
- [13] Joseph G Ellis, Brendan Jou, and Shih-Fu Chang. Why we watch the news: a dataset for exploring sentiment in broadcast video news. In *Proceedings of the 16th international conference on multimodal interaction*, pages 104–111, 2014. 2
- [14] Peihua Fu, Bailu Jing, Tinggui Chen, Jianjun Yang, and Guodong Cong. Modeling network public opinion propagation with the consideration of individual emotions. *International Journal of Environmental Research and Public Health*, 17(18):6681, 2020. 1
- [15] Shang-Hua Gao, Ming-Ming Cheng, Kai Zhao, Xin-Yu Zhang, Ming-Hsuan Yang, and Philip Torr. Res2net: A new multi-scale backbone architecture. *IEEE transactions on pattern analysis and machine intelligence*, 43(2):652–662, 2019. 3, 7
- [16] Hatice Gunes and Massimo Piccardi. A bimodal face and body gesture database for automatic analysis of human non-verbal affective behavior. In *18th International conference on pattern recognition (ICPR'06)*, volume 1, pages 1148–1153. IEEE, 2006. 2
- [17] Jad Haddad, Olivier Lézoray, and Philippe Hamel. 3d-cnn for facial emotion recognition in videos. In *Advances in Visual Computing: 15th International Symposium, ISVC 2020, San Diego, CA, USA, October 5–7, 2020, Proceedings, Part II 15*, pages 298–309. Springer, 2020. 3
- [18] Noushin Hajarolasvadi and Hasan Demirel. Deep emotion recognition based on audio–visual correlation. *IET Computer Vision*, 14(7):517–527, 2020. 3
- [19] Kevin A Hallgren. Computing inter-rater reliability for observational data: an overview and tutorial. *Tutorials in quantitative methods for psychology*, 8(1):23, 2012. 4
- [20] Kensho Hara, Hirokatsu Kataoka, and Yutaka Satoh. Can spatiotemporal 3d cnns retrace the history of 2d cnns and imagenet? In *Proceedings of the IEEE conference on Computer Vision and Pattern Recognition*, pages 6546–6555, 2018. 3, 7
- [21] Devamanyu Hazarika, Soujanya Poria, Amir Zadeh, Erik Cambria, Louis-Philippe Morency, and Roger Zimmermann. Conversational memory network for emotion recognition in dyadic dialogue videos. In *Proceedings of the conference. Association for Computational Linguistics. North American Chapter. Meeting*, volume 2018, page 2122. NIH Public Access, 2018. 7
- [22] Kaiping He, Xiangyu Zhang, Shaoqing Ren, and Jian Sun. Deep residual learning for image recognition. In *Proceedings of the IEEE conference on computer vision and pattern recognition*, pages 770–778, 2016. 3, 6, 7
- [23] Gao Huang, Zhuang Liu, Laurens Van Der Maaten, and Kilian Q Weinberger. Densely connected convolutional networks. In *Proceedings of the IEEE conference on computer vision and pattern recognition*, pages 4700–4708, 2017. 3
- [24] Alejandro Jaimes, Takeshi Nagamine, Jianyi Liu, Kengo Omura, and Nicu Sebe. Affective meeting video analysis. In *2005 IEEE International Conference on Multimedia and Expo*, pages 1412–1415. IEEE, 2005. 3
- [25] Shuiwang Ji, Wei Xu, Ming Yang, and Kai Yu. 3d convolutional

- tional neural networks for human action recognition. *IEEE transactions on pattern analysis and machine intelligence*, 35(1):221–231, 2012. 7
- [26] Yu-Gang Jiang, Baohan Xu, and Xiangyang Xue. Predicting emotions in user-generated videos. In *Proceedings of the AAAI conference on artificial intelligence*, volume 28, 2014. 2, 3, 5, 7
- [27] Abhinav Joshi, Ashwani Bhat, Ayush Jain, Atin Vikram Singh, and Ashutosh Modi. Cogmen: Contextualized gnn based multimodal emotion recognition. *arXiv preprint arXiv:2205.02455*, 2022. 7
- [28] Douwe Kiela, Edouard Grave, Armand Joulin, and Tomas Mikolov. Efficient large-scale multi-modal classification. In *Proceedings of the AAAI conference on artificial intelligence*, volume 32, 2018. 8
- [29] D Kollias and S Zafeiriou. Aff-wild2: Extending the aff-wild database for affect recognition. arxiv 2018. *arXiv preprint arXiv:1811.07770*. 2
- [30] Qiuqiang Kong, Yin Cao, Turab Iqbal, Yuxuan Wang, Wenwu Wang, and Mark D Plumbley. Panns: Large-scale pretrained audio neural networks for audio pattern recognition. *IEEE/ACM Transactions on Audio, Speech, and Language Processing*, 28:2880–2894, 2020. 3, 7
- [31] Ronak Kostl, Jose M Alvarez, Adria Recasens, and Agata Lapedriza. Emotion recognition in context. In *Proceedings of the IEEE conference on computer vision and pattern recognition*, pages 1667–1675, 2017. 1
- [32] Liliya Lavitas, Olivia Redfield, Allen Lee, Daniel Fletcher, Matthias Eck, and Sunil Janardhanan. Annotation quality framework-accuracy, credibility, and consistency. In *NEURIPS 2021 Workshop for Data Centric AI*, 2021. 3
- [33] Jiyoung Lee, Seungryong Kim, Sunok Kim, Jungin Park, and Kwanghoon Sohn. Context-aware emotion recognition networks. In *Proceedings of the IEEE/CVF international conference on computer vision*, pages 10143–10152, 2019. 2, 7
- [34] Shengzhe Liu, Xin Zhang, and Jufeng Yang. Ser30k: A large-scale dataset for sticker emotion recognition. In *Proceedings of the 30th ACM International Conference on Multimedia*, pages 33–41, 2022. 1, 3
- [35] Zhuang Liu, Hanzi Mao, Chao-Yuan Wu, Christoph Feichtenhofer, Trevor Darrell, and Saining Xie. A convnet for the 2020s. In *Proceedings of the IEEE/CVF conference on computer vision and pattern recognition*, pages 11976–11986, 2022. 3, 7
- [36] Ze Liu, Jia Ning, Yue Cao, Yixuan Wei, Zheng Zhang, Stephen Lin, and Han Hu. Video swin transformer. In *Proceedings of the IEEE/CVF conference on computer vision and pattern recognition*, pages 3202–3211, 2022. 2, 6, 7
- [37] John D Mayer, Peter Salovey, and David R Caruso. Mayer-salovey-caruso emotional intelligence test (msceit) users manual. 2002. 3
- [38] Bogdan Mocanu, Ruxandra Tapu, and Titus Zaharia. Multimodal emotion recognition using cross modal audio-video fusion with attention and deep metric learning. *Image and Vision Computing*, 133:104676, 2023. 3
- [39] Richard Orjeseck, Roman Jarina, Michal Chmulik, and Michal Kuba. Dnn based music emotion recognition from raw audio signal. In *2019 29th International Conference Radioelektronika (RADIOELEKTRONIKA)*, pages 1–4. IEEE, 2019. 7
- [40] Yagya Raj Pandeya and Joonwhoan Lee. Deep learning-based late fusion of multimodal information for emotion classification of music video. *Multimedia Tools and Applications*, 80:2887–2905, 2021. 2, 5, 7
- [41] Xiaokang Peng, Yake Wei, Andong Deng, Dong Wang, and Di Hu. Balanced multimodal learning via on-the-fly gradient modulation. In *Proceedings of the IEEE/CVF Conference on Computer Vision and Pattern Recognition*, pages 8238–8247, 2022. 3
- [42] Robert Plutchik. *The psychology and biology of emotion*. HarperCollins College Publishers, 1994. 2
- [43] Soujanya Poria, Erik Cambria, Devamanyu Hazarika, Navonil Majumder, Amir Zadeh, and Louis-Philippe Morency. Context-dependent sentiment analysis in user-generated videos. In *Proceedings of the 55th annual meeting of the association for computational linguistics (volume 1: Long papers)*, pages 873–883, 2017. 3
- [44] R Gnana Praveen, Patrick Cardinal, and Eric Granger. Audio-visual fusion for emotion recognition in the valence-arousal space using joint cross-attention. *IEEE Transactions on Biometrics, Behavior, and Identity Science*, 2023. 3
- [45] Flávio Ribeiro, Dinei Florencio, and Vítor Nascimento. Crowdsourcing subjective image quality evaluation. In *2011 18th IEEE International Conference on Image Processing*, pages 3097–3100. IEEE, 2011. 5
- [46] Liam Schoneveld, Alice Othmani, and Hazem Abdelkawy. Leveraging recent advances in deep learning for audio-visual emotion recognition. *Pattern Recognition Letters*, 146:1–7, 2021. 3
- [47] Dagmar Schuller and Björn W Schuller. The age of artificial emotional intelligence. *Computer*, 51(9):38–46, 2018. 1
- [48] Ajay S Singh and Micah B Masuku. Sampling techniques & determination of sample size in applied statistics research: An overview. *International Journal of economics, commerce and management*, 2(11):1–22, 2014. 5
- [49] P Soujanya, D Hazarika, N Majumder, G Naik, E Cambria, and R Mihalcea. A multimodal multi-party dataset for emotion recognition in conversations. 2018. 2
- [50] Du Tran, Lubomir Bourdev, Rob Fergus, Lorenzo Torresani, and Manohar Paluri. Learning spatiotemporal features with 3d convolutional networks. In *Proceedings of the IEEE international conference on computer vision*, pages 4489–4497, 2015. 3, 7
- [51] Minh Tran and Mohammad Soleymani. A pre-trained audio-visual transformer for emotion recognition. In *ICASSP 2022-2022 IEEE International Conference on Acoustics, Speech and Signal Processing (ICASSP)*, pages 4698–4702. IEEE, 2022. 3
- [52] Michel Valstar, Maja Pantic, et al. Induced disgust, happiness and surprise: an addition to the mmi facial expression database. In *Proc. 3rd Intern. Workshop on EMOTION (satellite of LREC): Corpora for Research on Emotion and Affect*, volume 10, page 65. Paris, France., 2010. 2
- [53] Ashish Vaswani, Noam Shazeer, Niki Parmar, Jakob Uszkoreit, Llion Jones, Aidan N Gomez, Łukasz Kaiser, and Illia Polosukhin. Attention is all you need. *Advances in neural information processing systems*, 30, 2017. 7

- [54] Chien-Yao Wang, Hong-Yuan Mark Liao, Yueh-Hua Wu, Ping-Yang Chen, Jun-Wei Hsieh, and I-Hau Yeh. Cspnet: A new backbone that can enhance learning capability of cnn. In *Proceedings of the IEEE/CVF conference on computer vision and pattern recognition workshops*, pages 390–391, 2020. [7](#)
- [55] Hui Wang, Siqi Zheng, Yafeng Chen, Luyao Cheng, and Qian Chen. Cam++: A fast and efficient network for speaker verification using context-aware masking. *arXiv preprint arXiv:2303.00332*, 2023. [7](#)
- [56] Kai Wang, Xiaojiang Peng, Jianfei Yang, Shijian Lu, and Yu Qiao. Suppressing uncertainties for large-scale facial expression recognition. In *Proceedings of the IEEE/CVF conference on computer vision and pattern recognition*, pages 6897–6906, 2020. [1](#)
- [57] Baohan Xu, Yanwei Fu, Yu-Gang Jiang, Boyang Li, and Leonid Sigal. Heterogeneous knowledge transfer in video emotion recognition, attribution and summarization. *IEEE Transactions on Affective Computing*, 9(2):255–270, 2016. [3, 7](#)
- [58] Baohan Xu, Yanwei Fu, Yu-Gang Jiang, Boyang Li, and Leonid Sigal. Video emotion recognition with transferred deep feature encodings. In *proceedings of the 2016 ACM on international conference on multimedia retrieval*, pages 15–22, 2016. [2, 5, 7](#)
- [59] Baohan Xu, Yingbin Zheng, Hao Ye, Caili Wu, Heng Wang, and Gufei Sun. Video emotion recognition with concept selection. In *2019 IEEE International Conference on Multimedia and Expo (ICME)*, pages 406–411. IEEE, 2019. [3, 7](#)
- [60] Ruize Xu, Ruoxuan Feng, Shi-Xiong Zhang, and Di Hu. Mmcosine: Multi-modal cosine loss towards balanced audio-visual fine-grained learning. In *ICASSP 2023-2023 IEEE International Conference on Acoustics, Speech and Signal Processing (ICASSP)*, pages 1–5. IEEE, 2023. [3](#)
- [61] Fanglei Xue, Zichang Tan, Yu Zhu, Zhongsong Ma, and Guodong Guo. Coarse-to-fine cascaded networks with smooth predicting for video facial expression recognition. In *Proceedings of the IEEE/CVF Conference on Computer Vision and Pattern Recognition*, pages 2412–2418, 2022. [3](#)
- [62] Jingyuan Yang, Jie Li, Leida Li, Xiumei Wang, and Xinbo Gao. A circular-structured representation for visual emotion distribution learning. In *Proceedings of the IEEE/CVF Conference on Computer Vision and Pattern Recognition*, pages 4237–4246, 2021. [1](#)
- [63] Quanzeng You, Jiebo Luo, Hailin Jin, and Jianchao Yang. Building a large scale dataset for image emotion recognition: The fine print and the benchmark. In *Proceedings of the AAAI conference on artificial intelligence*, volume 30, 2016. [3](#)
- [64] Yazhou Zhang, Mengyao Wang, Prayag Tiwari, Qiuchi Li, Benyou Wang, and Jing Qin. Dialoguellm: Context and emotion knowledge-tuned llama models for emotion recognition in conversations. *arXiv preprint arXiv:2310.11374*, 2023. [1](#)
- [65] Zhicheng Zhang, Lijuan Wang, and Jufeng Yang. Weakly supervised video emotion detection and prediction via cross-modal temporal erasing network. In *Proceedings of the IEEE/CVF Conference on Computer Vision and Pattern Recognition*, pages 18888–18897, 2023. [3, 6](#)
- [66] Sicheng Zhao, Yunsheng Ma, Yang Gu, Jufeng Yang, Tengfei Xing, Pengfei Xu, Runbo Hu, Hua Chai, and Kurt Keutzer. An end-to-end visual-audio attention network for emotion recognition in user-generated videos. In *Proceedings of the AAAI Conference on Artificial Intelligence*, volume 34, pages 303–311, 2020. [2, 3, 6, 7, 8](#)
- [67] Sicheng Zhao, Xingxu Yao, Jufeng Yang, Guoli Jia, Guiguang Ding, Tat-Seng Chua, Bjoern W Schuller, and Kurt Keutzer. Affective image content analysis: Two decades review and new perspectives. *IEEE Transactions on Pattern Analysis and Machine Intelligence*, 44(10):6729–6751, 2021. [1](#)
- [68] Hengshun Zhou, Debin Meng, Yuanyuan Zhang, Xiaojiang Peng, Jun Du, Kai Wang, and Yu Qiao. Exploring emotion features and fusion strategies for audio-video emotion recognition. In *2019 International conference on multimodal interaction*, pages 562–566, 2019. [2](#)